

Determination of buried active faults and earthquake potential for Izmir and its surroundings (western Turkey) using aeromagnetic anomalies and seismological data

Ezgi Erbek-Kiran^{*,1}, Abdullah Ates², Mustafa Nuri Dolmaz¹

⁽¹⁾ Suleyman Demirel University, Faculty of Engineering, Department of Geophysical Engineering, 32260, Isparta, Turkey

⁽²⁾ Ankara University, Faculty of Engineering, Department of Geophysical Engineering, 06100, Besevler, Ankara, Turkey

Article history: received June 28; 2022; accepted December 20, 2022

Abstract

The paper aims to delineate buried faults in Izmir city and its surroundings, western Turkey using aeromagnetic and seismological data. In this context, the geophysical data processing techniques including reduced-to-pole transform (RTP), power spectrum analysis, high-pass filter and second vertical derivative method (SVD) have been applied to the total field aeromagnetic data of the study area. First, to remove the undesirable effects caused by the dipolar nature of the Earth field, RTP transform has been applied to those data. Second, the average depths of the regional and residual sources in the region have been calculated as 16.84 km and 3.75 km, respectively using power spectrum analysis. After, to emphasize the effects of the residual anomalies, the high-pass filter has been applied to the RTP data. Finally, the second vertical derivative method (SVD) has been applied to the filtered data for delineating the uncovering buried faults and their lineaments in the eastern part of the Aegean extension. The results from those methods show five major fault zones that could cause devastating earthquakes in the area. Especially, the study reveals for the first time that one of these faults which lies from Doganbey to the city center of Izmir in the literature actually reaches out to Manisa city in the NE direction. As a result, these lineaments can be evaluated as traces of buried faults could be an important clue in predicting earthquake potential. A comparison of seismicity map and the heat flow map shows that the region (between Cesme and Seferihisar) represented with a low b-value has a high potential earthquake. The spatial distribution of the earthquakes, b-values and heat flow values in the depths may be related to the existence thin lithospheric mantle. Furthermore, the region represented by strong aeromagnetic anomalies may be considered to be magmatic material arising from the magma filling inside the strike-slip faults. The fault structure observed on the SVD map are also important for the geothermal energy potential of the region as well.

Keywords: Aeromagnetic data; Seismological data; Data-process; Second vertical derivative; Aegean region

1. Introduction

Aegean region is located on the western part of the Anatolian Plate, Turkey. The region is affected by different tectonic regimes such as crustal compression-extension, and retreatment along Hellenic trench [Mckenzie, 1972; Le Pichon and Angelier, 1979; Papazachos and Kiratzi, 1996]. It is well-established in the literature that the region is one of the most rapid expansiveness regions due to the extensional regime in the N-S direction. Researchers have suggested many arguments about the development of tectonism in the region. The most well-known of these arguments is the tectonic escape of the Anatolia plate to the westward direction proposed by Sengor [1979]. According to this argument, the movement has been caused by the subduction of the Africa plate beneath the Eurasia plate (through the Aegean-Cyprian Arc) and the continental collision of them. As a result of the collision, compression and extension region in the N-S direction have also been developed on the Anatolian Block. Hence, the counter clockwise rotational tectonic escapement in Western Anatolia has started in the late Miocene and continued to the present [Dewey and Sengor, 1979; Le Pichon and Angelier, 1979; Sengor and Yilmaz 1981; Sengor et al., 1985; Elitok and Dolmaz, 2008]. The extension rate of the region was defined as 14 ± 5 mm/year [Reilinger et al., 1997; McClusky et al., 2000].

In addition to the studies above, to define the crustal, tectonic and thermal structure of Western Anatolia, significant efforts have been performed in the literature. For example, Ates et al. [1999] compiled the aeromagnetic and gravity anomaly maps of Turkey. They suggested that the gravity anomalies in E-W directions located in the western part of Turkey could be related to the graben system in Western Anatolia. Then, Ates et al. [2012] determined the crustal thickness of Western Anatolia using aeromagnetic, gravity, and deep seismic reflection data. The thickness was calculated to be 34 km in the eastern part of Western Anatolia whereas it was found to be 25 km in the west of Western Anatolia. Dolmaz et al. [2005a] calculated the Curie point depths (CPD) of Western Anatolia through magnetic data and they showed that the estimated CPD values range from 9 km to 20 km. Duzgit et al. [2006] displayed that there is a correlation between the gravity and magnetic anomalies of Western Anatolia and the tectonic structures located in the region by utilizing the moving-windows application of Poisson's theorem. They showed that the relation between the negative correlation values and high heat flow was associated with asthenospheric upwelling. Bilim [2007] examined tectonic lineaments and thermal structure of the Kutahya-Denizli region (in Western Anatolia) by using aeromagnetic, gravity, and seismological data. Then, Bilim et al. [2016] calculated the CPD values and prepared heat flow maps for the Menderes Massif. Further, Erbek and Dolmaz [2019] examined the thermal structure and radiogenic heat production of the Aegean Sea and Aegean region through aeromagnetic data. They showed that the CPDs vary from 9.8 to 19.5 km whereas heat flow values vary between 50 and 125 mWm^{-2} . Besides those, the cross-gradient joint inversion method was applied to delineate the subsurface geology of the northern Menderes Massif by Gessner et al. [2016]. These joint inversions of gravity and magnetic anomaly data delineated primary tectonic domains and the extent of magmatic complexes in the upper crust of the northern Menderes Massif [Gessner et al., 2016]. Erbek [2021] carried out the structures and the basement depth estimation in the western Anatolia using aeromagnetic data and the study showed that the basement depths vary 1.4 km to 8.7 km beneath sea level.

The study area is located in the eastern part of the Aegean extension area around the towns of Izmir, Aydin and Manisa (Figure 1a). The region has crucial importance in terms of the major earthquake that occurred in the past. In addition, Izmir is a residential area and the third major city in Turkey. Therefore, this study aims at understanding the geo-hazards implications of these faults in the Bay of Izmir and its surrounding using aeromagnetic data. As well-known, the magnetic method is widely used in exploration geophysics from the past to the present. Especially airborne magnetic surveys are preferred by the researchers because they can be carried out on land, sea surface as well as air. Thus, it is regarded as a quick and effective way to explore the magnetization of the ground [e.g. Ates and Kearey, 1993].

Many studies focusing on the geological behaviour of this area have been completed in the literature while there are limited studies [Ates et al., 1999, 2009; Ates, 2015; Dolmaz et al., 2005a; Drahor and Berge, 2006; Bilim, 2007; Gonenc et al., 2012; Bilim et al., 2016; Dogru et al., 2017; Aydemir et al., 2018] using geophysical data processing methods including the methods (RTP transform, power spectrum analysis, high-pass filter, and SVD methods) used in this study. To contribute to this gap, this study concentrates on uncovering buried faults in the region as well as the active faults defined by using surface surveys in the literature. One way of delineating these areas is to use potential field data processing techniques [e.g. Ates and Kearey, 1993]. Furthermore, the magnetic method can be used to define the region in which magmatic material arises from the magma filling inside the strike-slip faults. The

Determination of buried active faults in Izmir and its surroundings (western Turkey)

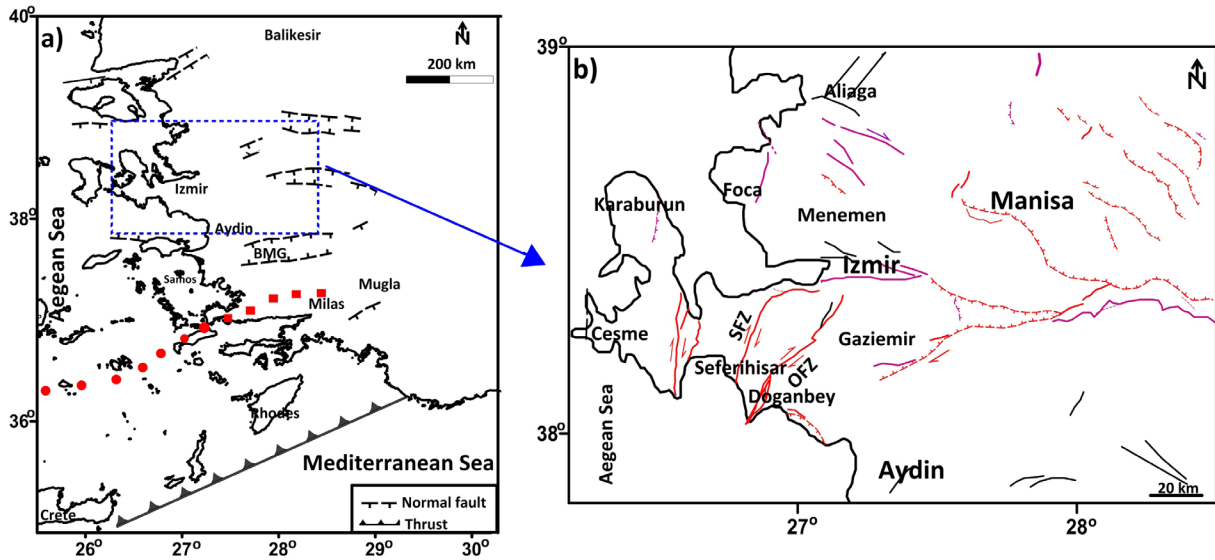


Figure 1. a) Generalized tectonic and location map of the study region [modified from Ates et al., 1997]. Red coloured dots and rectangulars show the Hellenic volcanic arc and its extension inland, respectively. Navy rectangle shows the research area. BMG: Buyuk Menderes Graben. b) Active fault map of the region [Modified from 1/1250000 digital active fault map of Mineral Research and Exploration General Directorate of the Republic of Turkey, Emre et al., 2013]. SFZ: Seferihisar fault zone, OFZ: Orhanli fault zone. Red colour: Holocene fault, Purple colour: Quaternary fault.

anomalies are in good agreement with the dyke-like bodies [defined by Tuncer et al., 1991] that elongate parallel to the fault line and they showed that the magnetized bodies causing magnetic anomalies filled into the faults that reach the magma. Considering all those outcomes obtained from the present study, this study has crucial importance for the region. Henceforth, this paper is organized as follows: Section 2 includes geological setting of the region. Section 3 describes the data and potential field data processing techniques. Section 4 provides the results with a discussion of methods used in the study. Section 5 concludes the paper and accommodates future suggestions about potential follow-up studies.

2. Geo-tectonic settings

The study region lies on the western end of the Menderes Massif (MM) and it contains one of the largest bay in the Aegean Sea known as the Bay of Izmir. In terms of geological and tectonic formations, the region covers the MM and Bornova Flysch Zone (BFZ-Bornova Mélange). As has been summarized in the previous section, tectonic regime has become effective in the occurrence of the E-W and NW-SE trending horst-graben system developing in the MM, Western Anatolia [Sengor and Yilmaz, 1981; Sengor et al., 1985; Bozkurt, 2001; Bozkurt and Sozbilir, 2004]. These graben systems are located on the MM known as the large metamorphic core complexes and they are filled with volcano-sedimentary units (Figure 2). It is divided into three sub-massifs as the northern, central and southern by the grabens (Gediz-Alasehir Graben, Buyuk Menderes Graben, Kucuk Menderes Graben) in E-W direction [Bozkurt and Sozbilir, 2004]. On the other hand, the MM is stratigraphically separated into two tectono-metamorphic units; core and cover rocks. The high-grade Augen gneisses which are under debate their origin in the region, are defined as the core rocks while Palaeozoic schist envelope and a Mesozoic to Cenozoic marble envelope are defined as the cover rocks [Rimmele et al. 2003]. In addition, the calculated radiometric ages of the geological units in the region are given in Figure 2.

The BFZ is defined as a regional olistostrome-mélange belt situated between the Izmir-Ankara Tethyan suture in the northwest and the MM in the southeast [Okay et al., 2012]. It includes blocks of Mesozoic limestone and ophiolite, which are bounded in Cretaceous-Palaeocene sheared sandstone and shale. These limestone blocks are collected in two types. The first consists of Late Triassic to Cretaceous shallow marine carbonates while the second

includes an Upper Triassic shallow marine section overlain by Jurassic to Cretaceous pelagic limestones [Okay et al., 2012]. Mesozoic limestone blocks are generally located in the north-western parts of the BFZ whereas ophiolitic blocks are located in the south-eastern of the BFZ (Figure 2). In addition, plutonic rocks located in the BFZ are associated with the extensional regime by Koralay et al. [2011], and their ages are determined as Pan-African, Triassic, and Miocene.

Another important geological structure in the region is Seferihisar High (Figure 2) which has two rises. The first rise consisted of Palaeozoic schists and Cretaceous units are located in the south while the second rise composed of Upper Cretaceous flysch is located in the northwest. Seferihisar fault zone (SFZ) and Orhanlı fault zone (OFZ) with the NE-SW orientation (Fig. 1b) are the major faults limiting Seferihisar High. Furthermore, the area is known as Seferihisar-Balcova geothermal (SBG) system in the literature. The thermal activity (average heat flow $\sim 110 \text{ mW m}^{-2}$) of the SBG has begun with the eruption of acid volcanics and it is demonstrated by hot springs that occur with the major fault systems [Esder and Simsek, 1975]. Besides the intrusive rocks, mapping of Miocene volcano-sedimentary units located in the Bay of Izmir indicates the existence of the two-phase volcanism. The oldest section includes calc-alkaline volcanic rocks with lower-middle Miocene ages while the younger section includes more magnetic rocks such as rhyolitic, pyroclastics etc. [Uzel and Sozibilir, 2008; Uzel et al., 2012].

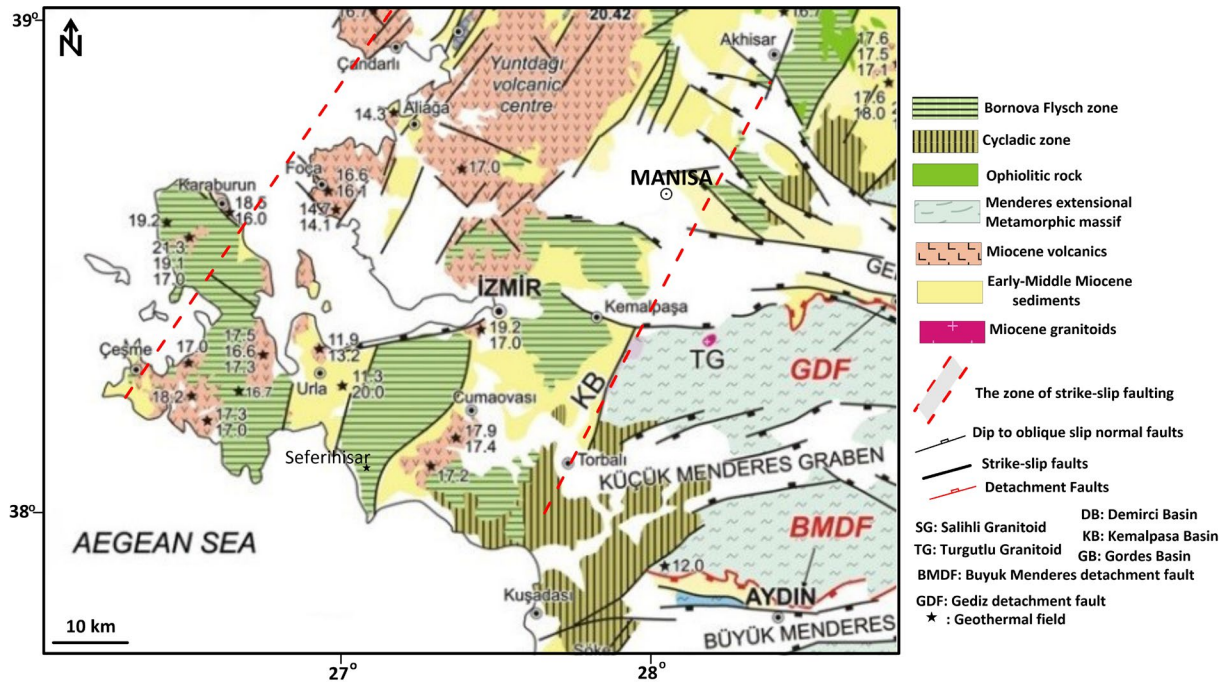


Figure 2. Simplified geological map of the study region [modified from by Sozibilir et al., 2011 and Ersoy et al., 2014]. Numbers on the map indicate the radiometric age of the geologic units.

3. Aeromagnetic data and geophysical data processing methods

This section covers the aeromagnetic data and mathematical definitions of the geophysical data processing methods used in this paper.

3.1 Aeromagnetic data

Aeromagnetic data used in this study are supplied from the General Directorate of the Mineral Research and Exploration Company of Turkey (MTA). These data were measured along N–S trending profiles spaced at 1-2 km intervals with 70 m sampling intervals and 600 m (approx. 2000 feet) flight altitude. All required correction on the

Determination of buried active faults in Izmir and its surroundings (western Turkey)

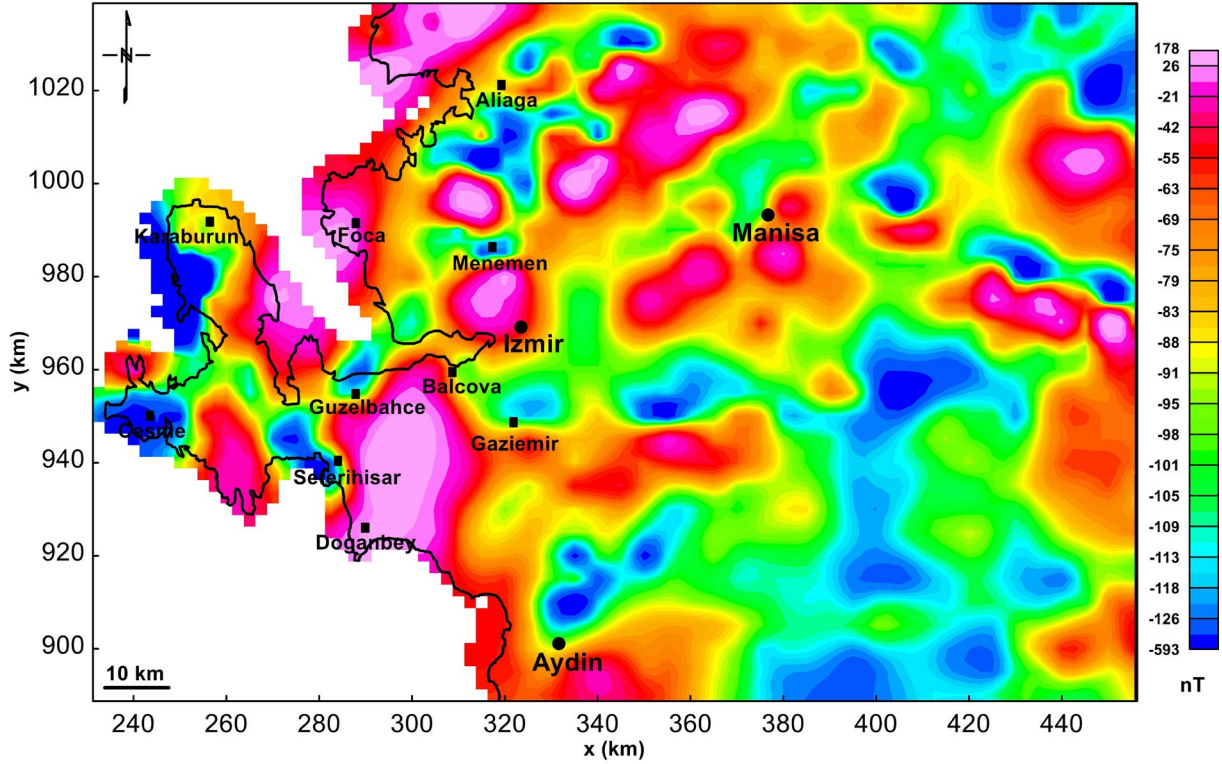


Figure 3. Distribution of aeromagnetic anomalies of the region.

aeromagnetic data were employed by MTA and the other technical details of data were mentioned in a previous study done by Ates et al. [1999]. They stated that the error tolerance in the data was 5%. Firstly, International Geomagnetic Reference Field (IGRF-1982.5) have been removed from the data. Then, the corrected data of the region have been gridded with a spacing of 5 km² (Figure 3).

The total field magnetic anomalies including short and long wavelength range from approximately -593 nT to +178 nT and a good relationship between the observed aeromagnetic anomalies and surface geology is seen. The negative anomalies are located in the eastern part of the region and west of the Karaburun Peninsula whereas the strong positive anomalies (approx. 170 nT) around the Seferihisar-Balçova trend. The other positive anomalies also align in NE-SW directions around the BFZ. The source of the positive anomalies located between Karaburun and Foca (located in the sea, see Aydemir et al. [2018]) might be associated with the volcanic units and intrusions in the outer Bay of Izmir.

On the other hand, the interpretation of magnetic data is a theoretically complex issue. This is caused by two main factors: the dipolar nature of the magnetic field and the magnetic response of the causative sources. This magnetic response of a given body changes according to location due to the variability of the geomagnetic field over the Earth's surface. Thus, the transformation from the total magnetic field data to the magnetic pole is an essential step for the interpretation of the magnetic data. This transform is known as the reduced-to-the-pole (RTP) transform [Baranov, 1957; Blakely, 1995; Macleod et al., 1993], in geophysical literature. RTP transform of the total magnetic intensity in wavenumber domain is formulated as;

$$A'(u, v) = \frac{A(u, v)}{(\sin I + i \cos I \cos(D - \theta))^2} \quad (1)$$

where $A(u, v)$ is amplitude at frequencies (u, v) , D and I are the geomagnetic inclination and declination of the magnetic field, respectively. θ is $\tan^{-1}\left(\frac{u}{v}\right)$. In this study, inclination and declination angles have been taken as 55° and 4°, respectively. By doing this transformation, the undesirable effects on the causative sources have been

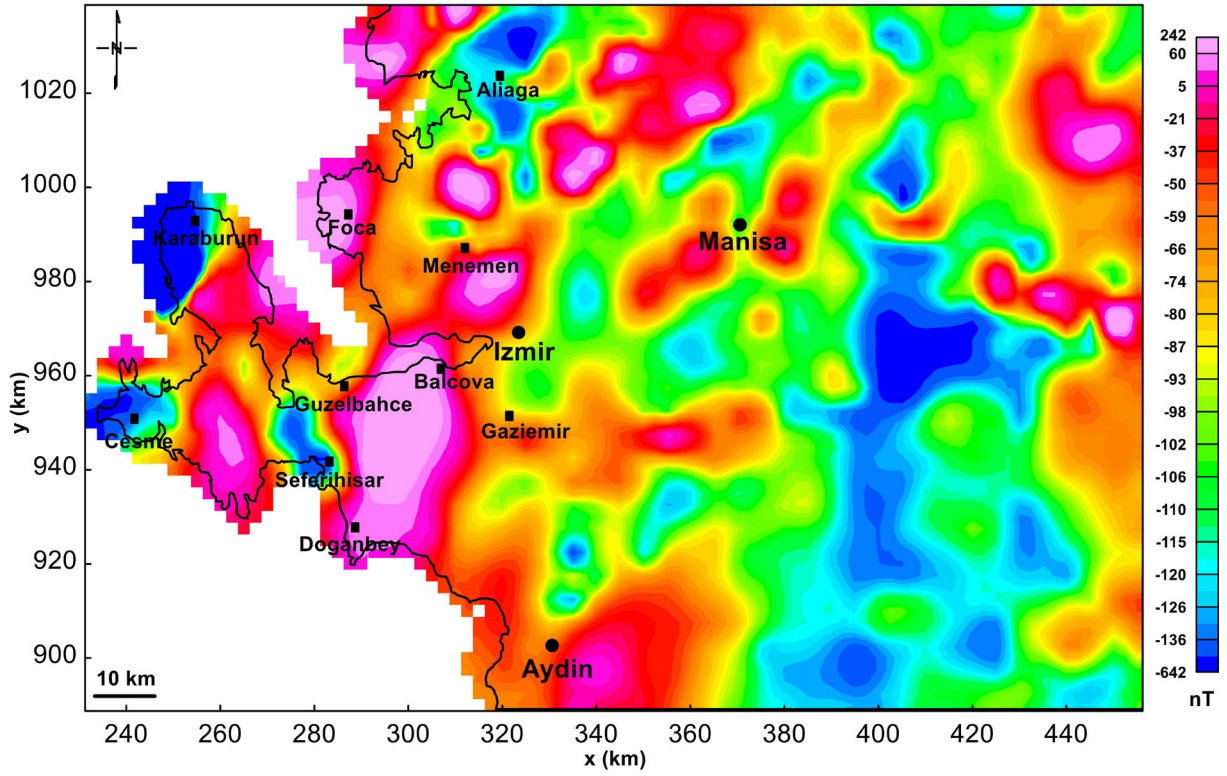


Figure 4. Reduced-to-pole transform map of the region.

removed from the aeromagnetic data. The data obtained as a result of this transformation has been illustrated in Figure 4. It indicates that the region extended from the Doganbey region to Manisa city displays a trend characterized by high aeromagnetic anomalies (approximately +240 nT).

3.2 Depth estimation of the causative sources

Power spectrum analysis has been the standard technique for potential field data processing in geophysics for a long time. The aeromagnetic data recorded in the geophysical survey are total magnetic fields generated by all subsurface sources. That is to say, the aeromagnetic data include both types of anomalies caused by shallow sources and deeper sources. Especially in small-scale research, the magnetic responses of sources buried at shallow depths are often suppressed by regional anomalies caused by deeper structures. Therefore, the determination of the depth of these causative sources could be difficult in the potential field data interpretation. To overcome this issue, in our study, the power spectrum analysis developed by Spector and Grant [1970] is used to calculate the average depth of the regional and residual anomalies. A given potential field function in the space domain has a single and unique wavenumber domain function, and vice versa. The addition of two functions (anomalies) in the space domain is equivalent to the addition of their transforms. In other words, the method uses the Fast Fourier Transform (FFT). The mathematical expression of the power spectrum is given as;

$$P(w) \sim e^{-wh} \tag{2}$$

where, h is the depth of the source and w is the wavenumber [Yadav et al., 2018]. The energy spectrum is a 2D function of the energy relative to wavenumber and direction. The radially averaged energy spectrum is a function of the wavenumber alone and is calculated by averaging the energy for all directions for the same wavenumber. As can be seen from eq. (2), the power spectrum is directly related to depth. The averaged depths of the causative

Determination of buried active faults in Izmir and its surroundings (western Turkey)

sources in the considered area are calculated by using the slope of the log radially averaged power spectrum. The depth obtained from the linear relationship between wavenumber and logarithmic power spectrum of the data is expressed as:

$$h = -\frac{S}{4\pi} \quad (3)$$

where S is the slope of the logarithmic power spectrum. This analysis is used widely to determine lithological units and their boundaries.

Figure 5 indicates the average depths of each segment in the region. The figure could be divided into three segments. The first segment includes frequencies that range from 0.001 to 0.014 cycle/km. This segment represents the regional anomalies caused by the deeper magnetized sources. The second segment contains frequencies vary between 0.015 and 0.049 cycle/km. The average depths of deeper magnetized sources (D1) and intermediate magnetized sources (D2) have been calculated as 16.84 km and 8.39 km, respectively. The third segment represents the shallow magnetized sources characterized by the short wavelengths in the region. This segment could be associated with the magnetic bodies (like igneous and metamorphic) that are emplaced into the basement underlying the sedimentary cover. Also, the average depth of these shallow sources has been calculated as 3.75 km.

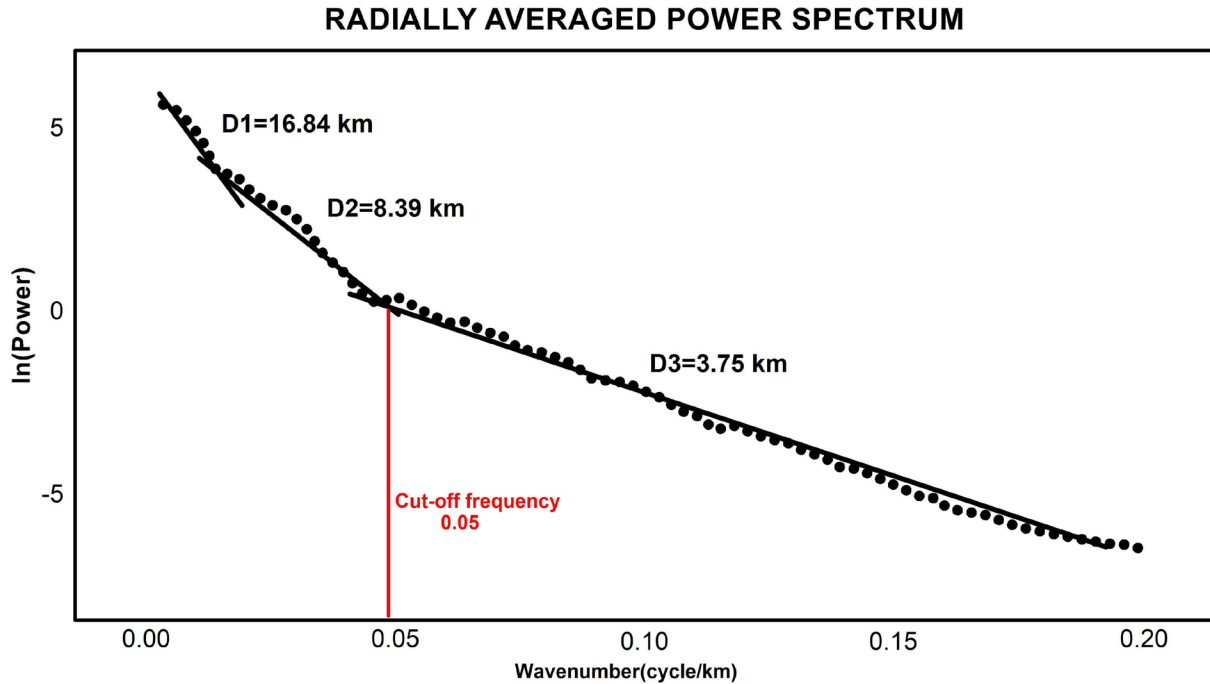


Figure 5. Radially averaged power spectrum of the considered area. The power spectrum shows three sources at depths ranging from 3.75 to 16.84 km.

3.3 High-pass filtering anomalies

Filtration has a key role in the interpretation of the data. In the literature, there are different filter choices such as low-pass filter, high-pass filter, band-pass filter, Butterworth filter. In this study, we used the high pass filter for the RTP magnetic data. The high-pass filters are often used to emphasize the details of the shallow effects in the upper crust. In other words, the effects stem from deep sources are removed from the total field anomaly by applying the high-pass filter.

The high-pass aeromagnetic filtered map with frequency cut off 0.05 cycle/km (Figure 6) includes many strong anomalies. Most of these anomalies with NE-SW trending located in the onshore area and they start the Doganbey

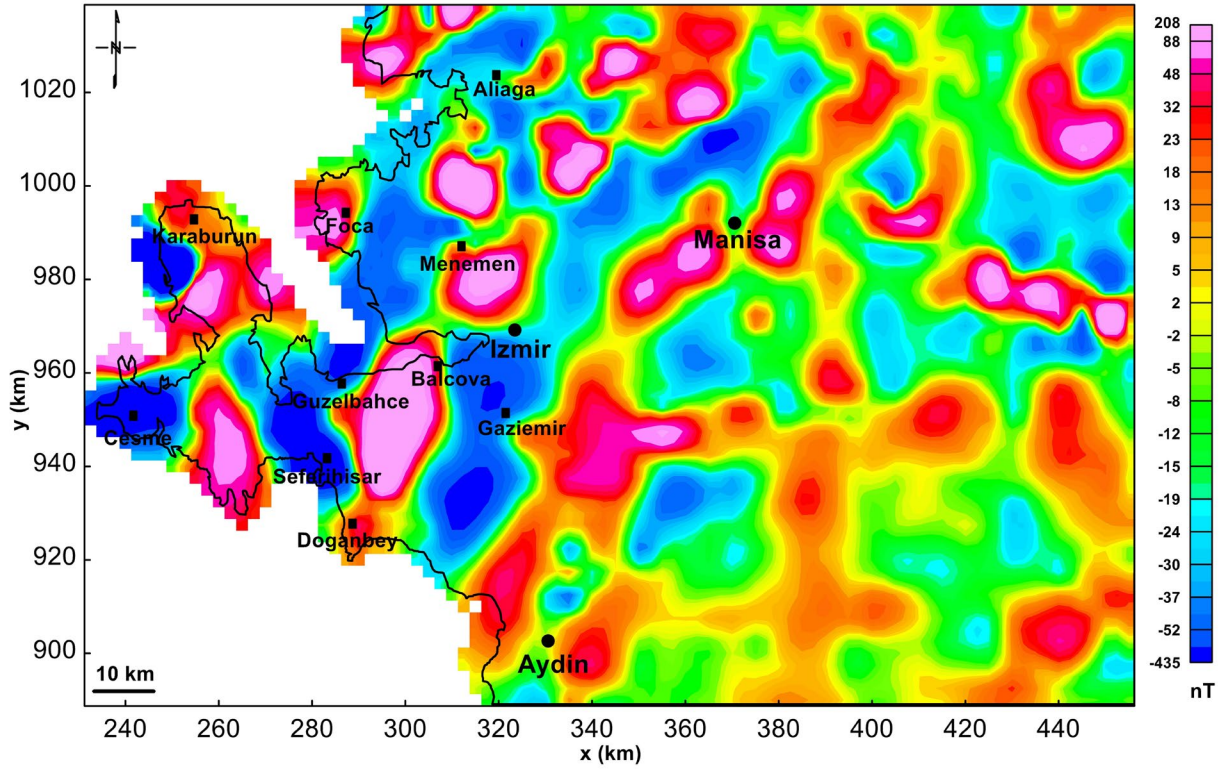


Figure 6. High-pass filtered aeromagnetic anomalies in the considered region. Cut-off frequency is 0.05 cycles/km.

and continue from east of Aliaga. These high magnetic anomalies in the map correspond to Seferihisar high (Bornova Flysch zone) and Yuntdagı volcanic center in the geology map (see Figure 2). Besides these, the negative anomalies located in the eastern part of Seferihisar High are probably caused by the Neogene-Quaternary fill sediments (see Figure 2).

3.4 Second vertical derivative method (SVD)

Derivative methods (horizontal and vertical gradient methods) are expected to enhance causative source boundaries in anomaly maps. In other words, the method provides a better view for us to interpret anomalies that are often important in geophysical surveys. The first-order Fourier transformation was first proposed by Blakely [1995] and it is given as;

$$F = \left[\frac{\partial P}{\partial Z} \right] = |k|F|P| \quad (4)$$

where P is the potential field data, k is wavenumbers. Similar to equation 4, the nth-order vertical derivative can be calculated as follows;

$$F = \left[\frac{\partial^n P}{\partial Z^n} \right] = |k|^n F|P| \quad (5)$$

The SVD of potential field data has been used as a tool for delineation the boundaries of causative sources in geologic interpretations or geophysical investigations since the early 1950s [Sumintadireja et al., 2018]. Further, the SVD is often used to reveal geological structures which are especially normal or reverse faults.

Determination of buried active faults in Izmir and its surroundings (western Turkey)

In this study, the SVD method has been applied to filtered the RTP data due to the usefulness in revealing the causative sources geometry. By a closer look at Figure 7, it has been seen that the effect of shallow sources is enhanced in the SVD map. It is also noticed that the boundaries of the several structures which lie on the NE-SW directions are detected in the region. In addition, a remarkable anomaly is observed in the Karaburun peninsula. It starts from Cesme and runs to the Bay of Izmir nearly E-W trending. Another anomaly is also located in Seferihisar High.

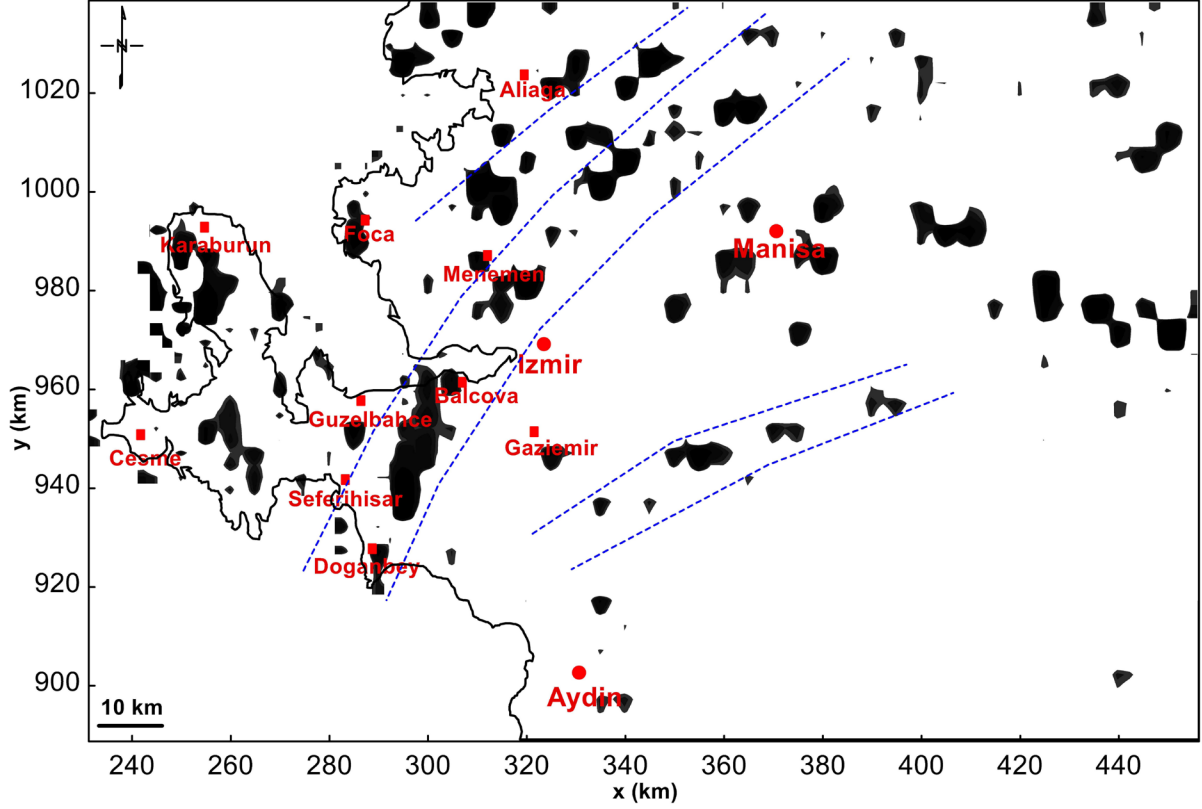


Figure 7. The second vertical derivative anomalies of the filtered aeromagnetic data. The regions shown by the navy-coloured dashed lines is defined as the fault zones.

3.5 Seismological data

Earthquakes used in this study are obtained from the KOERI (Kandilli Observatory and Earthquake Research Institute). A version of this earthquake catalogue is available at <http://www.koeri.boun.edu.tr/sismo/zeqdb/>. The dataset contains the earthquakes whose focal depths reach 100 km occurred between the years 1964 and 2021 in the Aegean region of Turkey. In order to obtain a uniform earthquake catalogue, body-wave magnitude (M_b) and surface magnitude (M_s) have been converted to moment magnitude (M_w) utilizing below empirical relations developed by Scordilis [2006].

$$M_w = 0.67 (\pm 0.005) M_s + 2.07 (\pm 0.03), \quad 3.0 \leq M_s \leq 6.1 \quad (6)$$

$$M_w = 0.99 (\pm 0.02) M_s + 0.08 (\pm 0.13), \quad 6.1 \leq M_s \leq 8.2 \quad (7)$$

$$M_w = 0.85 (\pm 0.04) M_b + 1.03 (\pm 0.23), \quad 3.5 \leq M_b \leq 6.2 \quad (8)$$

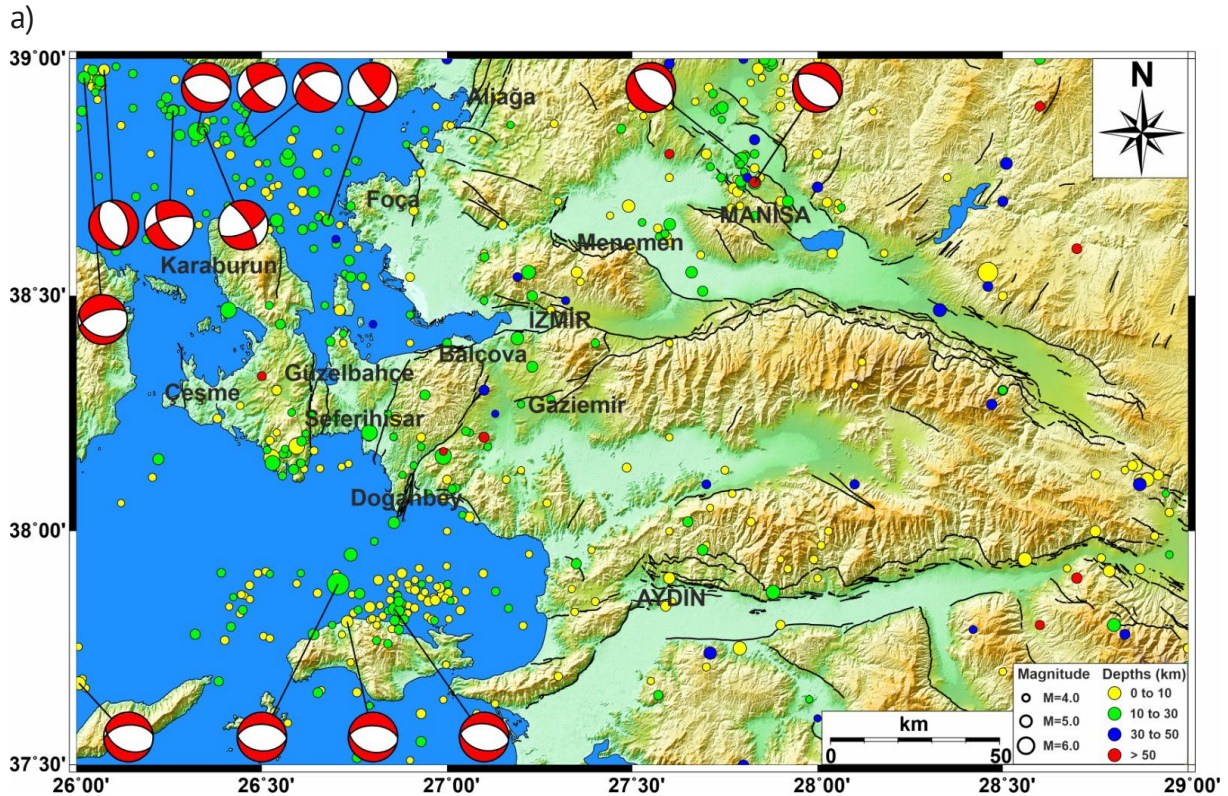


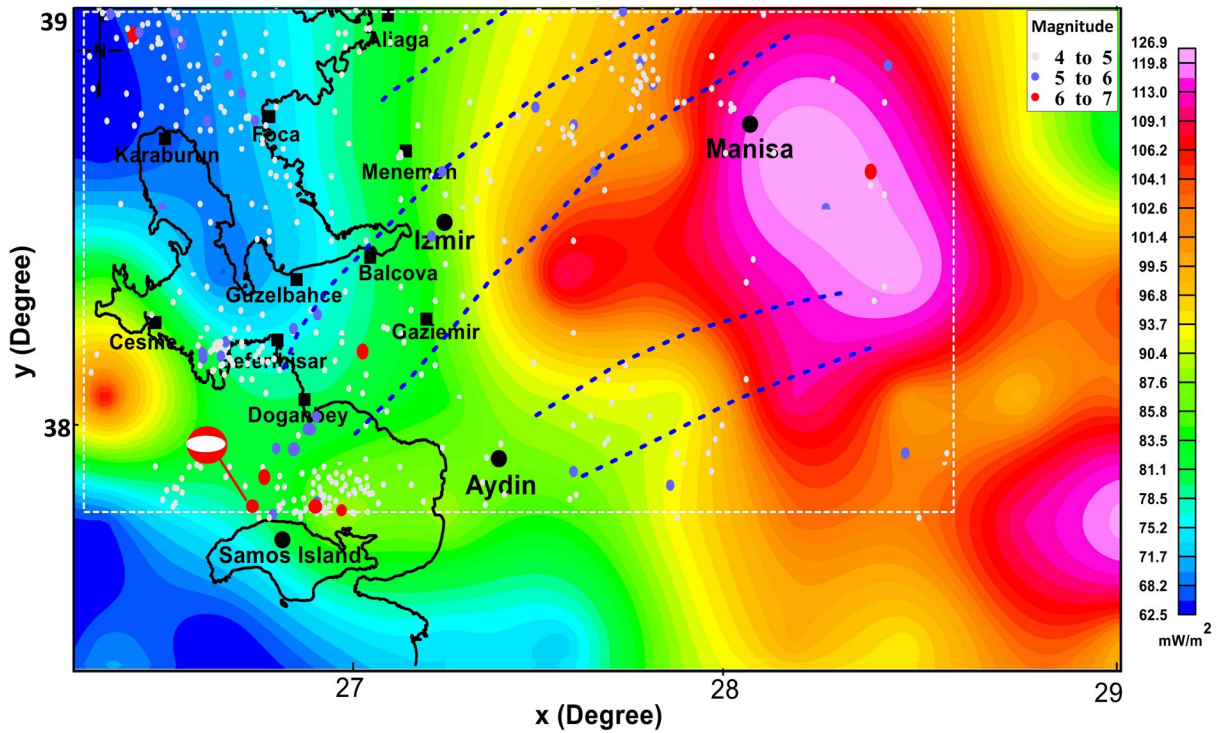
Figure 8. a) The seismicity map of study region. The fault mechanism solutions of the major earthquakes are shown for the region. Focal mechanisms are taken from the Disaster and Emergency Management Authority (AFAD) and the active fault map modified from Emre et al. [2013].

In this section, the study area is expanded a little more and it is aimed to better interpret the tectonic implications in the region. We analysed 538 earthquakes with magnitudes ranging from $4.0 \leq M \leq 7.0$ that occurred in the study area. The distribution of these earthquakes is given in Figure 8a. The map shows that the occurrence of the earthquakes follows the line in NE-SW directions (from Doganbey to the north of Manisa). The magnitudes of these earthquakes vary between 4 and 5 inland parts of the region while the earthquakes that magnitudes reach up to 7 have occurred in coastal and offshore regions. The focal depths of earthquakes (Figure 8a) indicate that approximately 92.4% of the earthquakes have occurred at depths of 0-30 km in the crust. Also, the distribution of earthquake focal depths showed that the offshore earthquakes generally occurred at shallow depths (Figure 8a). For instance, the focal depth the Samos Island earthquake ($M = 6.6$), which occurred on an E-W trending low-angle normal fault passing through the north of Samos Island (see Figure 8a), is determined as 14.9 km (AFAD, 2020). This earthquake caused deaths and destruction of buildings in İzmir.

The understanding of the crust structure and its properties has an important issue in terms of the tectonic and seismic activity. Also, the distribution of the temperature within the earth's crust affects the active tectonics and seismicity [Bott 1982]. Previous studies carried out on the thermal structure in the region [Jongsma 1974; Fytikas 1980; Erbek and Dolmaz 2019] show that the Aegean region is characterized by higher than average continental heat-flow values because of the back-arc nature of the region. In Figure 8b, the heat flow map was extracted from previous study carried out by Erbek and Dolmaz [2019]. The heat flow values vary between 65 and 120 mW/m². By a closer look at Fig. 8b, it is observed that the Karaburun peninsula is represented with low heat flow values whereas the southern part of Cesme and the continental Aegean region (Western Anatolia) are represented with high heat flow values. Also, a comparison of the earthquake map (Figure 8a) and the heat flow map (Figure 8b) revealed that low seismicity is in good agreement with high heat flow. In addition, the transition from seismic zone to a-seismic zone may be evaluated as a thermal effect [Hyndman and Wang 1993; Dolmaz et al. 2005b]. Hence, this relation makes a more ductile region in the crust. Similarly, Dolmaz et al. [2005b] interpreted that low seismic activity within the regionally active seismic areas seems to be associated with high heat flow (shallow Curie Point Depth). Besides those, in the present study, (such as the Orhanlı fault and Seferihisar fault zones). Also, the thermal structure of

Determination of buried active faults in Izmir and its surroundings (western Turkey)

b)



c)

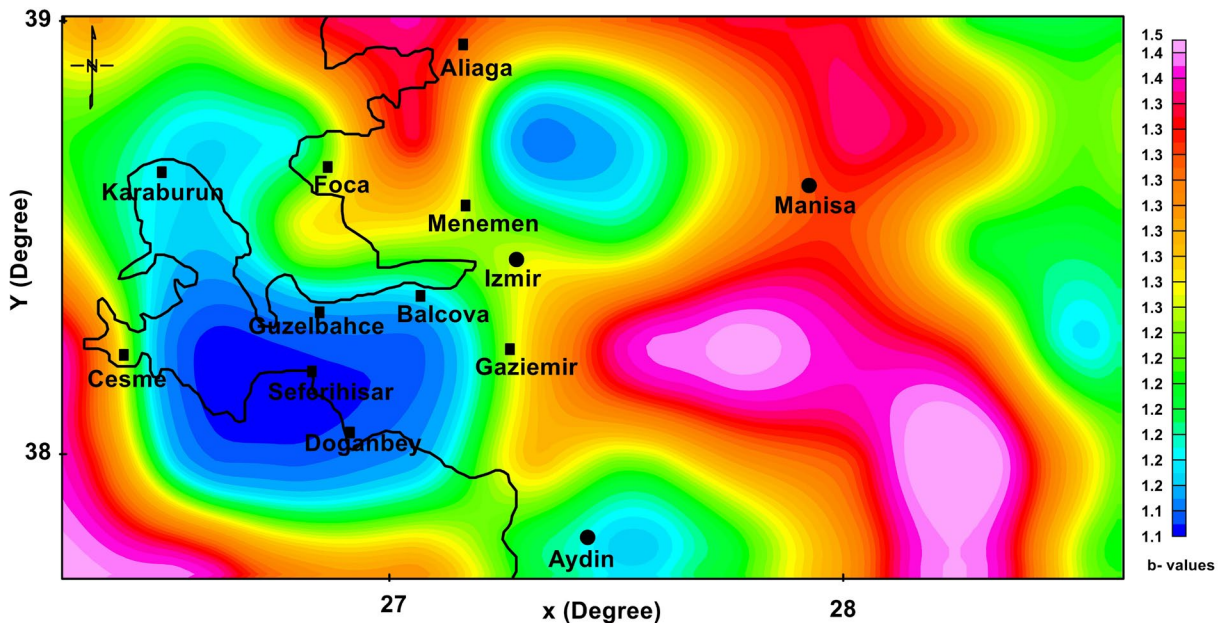


Figure 8. b) Heat flow map from Erbek and Dolmaz [2019]. The white rectangle indicates the selected region for the calculation of the b-values c) b-value map.

the region and intense seismicity have important role for the selected region. b-values, which can be identified as indirect indications of the rheological features of the earth's materials under stress and strain, are calculated from the Gutenberg–Richter relation for the selected region using the least-square procedure and accepted constant [Kalyoncuoglu et al. 2013]. The stress and strain areas of the region have been determined utilizing b-value map (Figure 8c). The stress and strain have an inverse relation with the b-value. In other words, when the stress and strain increase, the b-value decreases. According to this relation, Figure 8c showed that the region located between Cesme and Seferihisar is under high stress and strain.

4. Discussions

The recorded aeromagnetic data have been refined using geophysical data processing. The RTP transform has been applied to aeromagnetic data in order to remove the undesirable effects caused by the dipolar nature of the magnetic field and the superposition of magnetic sources. After, based on previous studies made so far in the region, the lineaments of the major faults located in the western part of the Aegean extension area have been investigated in detail using aeromagnetic data. Recently produced maps (the RTP transform, the high-pass filter and SVD maps) have supplied important information for the region (see Figures 4, 6 and 7). Observing the RTP magnetic anomaly map (Fig. 4) shows that there is a correlation between the area characterized by high amplitude magnetic anomalies and the outcrops of Bornova Flysch Zone (BFZ) and Miocene volcanics (Figure 2). Also these high magnetic anomalies correspond to the zone of strike-slip faulting mapped in Figure 2. Another large anomaly located on the north of Doganbey extends to Balçova. This anomaly corresponds to the Seferihisar High included the units of BFZ. Furthermore, this strong anomaly is also observed in the high-pass filter map and the SVD map (see Figures 6 and 7). On the other hand, the centre of the Menderes Massif has displayed lower negative magnetic anomalies. It is thought that this massif lost its magnetization feature because it had a very blended and complex structure throughout history. In order to interpret of the magnetic data in detail, the power spectrum analysis has been applied to RTP data. By doing so, the average depths of the deeper and shallower magnetized bodies have been calculated as 16.84 km and 3.75 km, respectively (see Figure 5). By applying the high-pass filter and the SVD methods, the anomalies caused by shallow effects in the upper crust have been emphasized in the details (Figures 6 and 7). By a closer look at Figure 7, the SVD map shows the lineaments (marked by navy colour) determined for the region. These lineaments (see Figure 7) have been drawn according to the findings obtained from the SVD map. As can be known, the SVD method is widely used in the estimate fault structure and emphasize shallower geologic anomalies. In this context, the SVD map produced in this study has provided valuable information about fault lineaments. The strong magnetic anomalies that are caused by magmatic material arising from the magma filling inside the strike-slip faults could be evaluated (Figure 7). Therefore, it could be considered that these lineaments may be the indicator of the fault structure.

On the other hand, the distribution of the earthquakes was correlated with the SVD map. Interpretation of this correlation was shown that earthquakes occurred in the regions showing with the blue line in the SVD map. By examining the epicentres of earthquakes, it has been seen that earthquakes occur in a trend. Also, the earthquakes that occurred offshore the Doganbey (northern edge of Samos island) take attention in Figure 8a. Since this study does not include the marine data, we utilized the previous study carried by Erbek and Dolmaz [2019] in order to interpret the earthquakes that occurred in the offshore region. This region is characterized by high magnetic anomalies. It is thought that this phenomenon may be related to the existence of a fault system located between Doganbey and Samos that has not been recognized yet. Also, considering the previous studies [Kalyoncuoglu et al., 2013; Oruc and Balkan, 2021] in the region, the spatial distribution of the earthquakes, b-values and heat flow values in these depths may be related to the existence thin lithospheric mantle. Furthermore, the low NE-SW trending b-value anomaly zone in region between Cesme-Doganbey shows the increase in stress accumulation (see Figure 8c) caused by the westward and counter clockwise rotation movement in this area. In other words, these movements in western Anatolia and the Aegean Sea increase the stress energy on the faults and it causes observing low b-values.

In addition to those, the fault that lies through Izmir to Manisa cannot be observed in an active fault map [Emre et al., 2013] and the surface geology. However, this study reveals for the first time that a buried fault shows existence in the region covered by Doganbey, İzmir and Manisa (see Figure 7). Also, this exploration could be an indication of the fact that that the possible geothermal energy sources might take place in this region.

5. Conclusions

The existence of magnetized upper crust or crustal substances can be seen by airborne magnetic surveys on the aeromagnetic anomaly maps. The aeromagnetic anomalies provided by MTA have been used in this study to reveal the trace buried faults that can be significant for predicting the earthquake potential. By a closer look at Figs. 4, 6, 7 it can be seen that intense positive anomalies aligned along the faults. Besides those, the recently re-prepared active fault map of Turkey [Emre et al. 2013] shows strike-slip faults elongated along the NE-SW direction towards Izmir city (Fig. 1b). One of the faults can be observed towards Izmir. Although on the active fault map this fault cannot be

Determination of buried active faults in Izmir and its surroundings (western Turkey)

observed beyond northeast of Izmir, its existence can be traced, from the aeromagnetic anomalies, through Izmir to Manisa. As a conclusion, the comparison of the results obtained from the SVD map and available active fault map produced by MTA shows that the results are generally consistent with each other. The other lineaments marked on Figure 7 are also located in the Karaburun Peninsula and NE of Aydın city. However, the same observations in Figure 7 are not valid for Fig.1b. Accordingly; these lineaments have been discovered by using geophysical data processing and they have been recognized for the first time in this study.

In addition, seismicity in the region was investigated in detail. The SVD map and the earthquake distribution map are superimposed on each other. The map (Figure 8a) indicated that earthquakes occurring in Western Anatolia occurred in the areas bounded by dark blue dashed lines. Also, seismicity was compared with the thermal structure and b-value distribution. Especially, the b-value map (Figure 8c) showed that the region (between Cesme and Seferihisar) is represented with a low b value has a high potential earthquake. Therefore, we suggest that the regions delineated by the results of the present study should furthermore be supported by geophysical studies in the future.

Data availability. The presented aeromagnetic data were recorded by the General Directorate of the Mineral Research and Exploration (MTA). This original data remains confidential and the property of MTA.

Acknowledgment. The aeromagnetic data of the study region were obtained from the General Directorate of the Mineral Research and Exploration (MTA) of Turkey.

References

- AFAD (2020). Türkiye İvme Veri Tabanı ve Analiz Sistemi (TADAS) (Version 1.3), Deprem Dairesi Başkanlığı, Afet ve Acil Durum Yönetimi Başkanlığı (AFAD), <https://tadas.afad.gov.tr>.
- Ates, A. and P. Kearey (1993). Deep structure of the East Mendip Hills from gravity, aeromagnetic and seismic reflection data, *J. Geol. Soc. London*, 150, 1055-1063.
- Ates, A., A. Sevinc, Y.K. Kadioglu and P. Kearey (1997). Geophysical investigations of the deep structure of the Aydın-Milas region, southwest Turkey: Evidence for the possible extension of the Hellenic Arc, *Israel J. Earth Sci.*, 46, 1, 29-40.
- Ates, A., P. Kearey and S. Tufan (1999). New gravity and magnetic maps of Turkey, *Geophys. J. Int.*, 136, 499-502.
- Ates, A., A. Buyuksarac, F. Bilim, O. Bektas, C. Sendur and G. Komanovali (2009). Spatial correlation of the aeromagnetic anomalies and seismogenic faults in the Marmara region, NW Turkey, *Tectonophysics*, 478, 135-142.
- Ates, A., F. Bilim, A. Buyuksarac, A. Aydemir, O. Bektas and Y. Aslan (2012). Crustal structure of Turkey from aeromagnetic, gravity and deep Seismic reflection data, *Surv. Geophys.*, 33, 869-885.
- Ates, A., 2015. Correlation of faults with airborne magnetic anomalies of Gulf of Izmir and surrounding, western Turkey. *International Conference on Environmental Science and Technology (ICOEST-2015)*, 9-13 Sep.2015, Sarajevo. Bosnia and Herzegovina, Abstract Proceedings, 28.
- Aydemir, A., F. Bilim, G. Cifci and S. Okay (2018). Modeling of the Foca-Uzunada magnetic anomaly and thermal structure in the gulf of Izmir, western Turkey, *J. Asian Earth Sci.*, 156, 288-301.
- Baranov, V., 1957, A new method for interpretation of aeromagnetic maps: pseudo-gravimetric anomalies, *Geophysics*, 22, 359-383.
- Bilim, F. (2007). Investigation into the tectonic lineaments and thermal structure of Kutahya-Denizli region western Anatolia, from using aeromagnetic, gravity and seismological data, *Phys. Earth Planet. Inter.*, 165, 135-146.
- Bilim, F., T. Akay, A. Aydemir and S. Kosaroglu (2016). Curie point depth, heat-flow and radiogenic heat production deduced from the spectral analysis of the aeromagnetic data for geothermal investigation on the Menderes Massif and the Aegean Region, Western Turkey, *Geothermics*, 60, 44-57.
- Blakely, R.J. (1995). *Potential theory in gravity and magnetic applications*. Cambridge University Press, NY, USA, 441.
- Bott, M.H.P. (1982). *The interior of the earth: its structure constitution and evolution*. Edward Arnold, London, 316.
- Bozkurt, E. (2001). Neotectonics of Turkey-a synthesis, *Geodinamica Acta*, 14, 3-30.
- Bozkurt, E. and H. Sozbilir (2004). Tectonic evolution of the Gediz Graben: field evidence for an episodic, two-stage extension in western Turkey, *Geol. Mag.*, 141, 63-79.

- Dewey, J. and C. Sengor (1979). Aegean and surrounding regions complex multiplate and continuum tectonics in a convergent zone, *Geol. Soc. Am. Bull.*, 90, 84-92.
- Dogru, F., O. Pamukcu and I. Ozsoz (2017). Application of tilt angle method to bouguer gravity data of western Anatolia, *Bull. Mineral Res. Expl.*, 155, 213-222.
- Dolmaz, M.N., Z.M. Hisarli, T. Ustaomer and N. Orbay (2005a). Curie point depths based on spectrum analysis of the aeromagnetic data, West Anatolian extensional province, Turkey, *Pure Appl. Geophys.*, 162, 571-590.
- Dolmaz, M.N., T. Ustaomer, Z.M. Hisarli and N. Orbay (2005b). Curie Point Depth variations to infer thermal structure of the crust at the African-Eurasian convergence zone, SW Turkey, *Earth Planet Spa.*, 57, 373-383.
- Drahor, M. and A.M. Berge (2006). Geophysical investigations of the Seferihisar geothermal area, Western Anatolia, Turkey, *Geothermics*, 35, 302-320.
- Duzgit, Z., Z.M. Hisarli, N. Sayin and N. Orbay (2006). Correlation between gravity and magnetic anomalies of Western Anatolia and its relation to tectonic structures, *Earth Planet Spa.*, 5, 943-949.
- Elitok, O. and M.N. Dolmaz (2008). Mantle flow-induced crustal thinning in the area between the easternmost part of the Anatolian plate and the Arabian Foreland (E Turkey) deduced from the geological and geophysical data, *Gondwana Res.*, 13, 302-318.
- Emre, O, T.Y. Duman, S. Ozalp, H. Elmaci, S. Olgun and F. Saroglu (2013). Active fault map of Turkey with an Explanatory Text. 1/1,250,000 scale, General Directorate of Mineral Research and Exploration, Special Publication Series-30, Ankara-Turkey. ISBN: 978-605-5310-56-1 <https://www.mta.gov.tr/en/maps/active-fault-1250000>.
- Erbek, E. and M.N. Dolmaz (2019). Investigation of the thermal structure and radiogenic heat production through aeromagnetic data for the south-eastern Aegean Sea and western part of Turkey, *Geothermics*, 81, 113-122.
- Erbek, E. (2021). An investigation on the structures and the basement depth estimation in the western Anatolia, Turkey using aeromagnetic data. *Geosci. J.* <https://doi.org/10.1007/s12303-021-0001-y>.
- Ersoy, E.Y., I. Cemen, C. Helvacı and Z. Billor (2014). Tectono-stratigraphy of the Neogene basins in Western Turkey: implications for tectonic evolution of the Aegean extended region, *Tectonophysics*, 635, 33-58.
- Esder, T. and S. Simsek, (1975). Geology of İzmir (Seferihisar) geothermal area western Anatolia of Turkey determination of reservoirs by means of gradient drilling. *Proceedings of 2nd UN Symposium, San Francisco*, 349-361.
- Fytikas, M.D. (1980). Geothermal exploitation in Greece. 2 nd Int. Sem on the results of E.C. Geothermal Energy Research, Strasbourg. In: Strub AS and Ungemach P (Eds) pp. 213-237, Reidel Publ. Dordrecht.
- Gessner, K., L.A. Gallardo, F. Wedin and K. Sener (2016). Crustal structure of the northern Menderes Massif, western Turkey, imaged by joint gravity and magnetic inversion, *Int. J. Earth Sci.*, 105, 2133-2148.
- Gonenc, T., O. Pamukcu, C. Pamukcu and A.H. Deliormanli (2012). The investigation of hot spots in western Anatolia by geophysical and mining approaches, *Energy Sources*, 34, 775-792.
- Hyndman, R.D. and K. Wang (1993). Thermal constraints on the zone of possible major thrust earthquake failure on the Cascadia subduction zone, *J. Geophys. Res.*, 98, 2039-2060.
- Jongsma, D. (1974). Heat flow in the Aegean Sea, *Geophys. J. Int.*, 37, 3, 337-346.
- Kalyoncuoglu, U.Y., O. Elitok and M.N. Dolmaz (2013). Tectonic Implications of Spatial Variation of b-Values and Heat Flow in the Aegean Region, *Marine Geophys. Res.*, 34, 59-78.
- Koralay, O.E., O. Candan, C. Akal, O.O. Dora, F. Chen, M. Satir and R. Oberhansli (2011). The geology and geochronology of the Pan-African and Triassic metagranitoids in the Menderes Massif, Western Anatolia, Turkey, *Bull. Mineral Res. Explor.*, 142, 39-121.
- Le Pichon X. and J. Angelier (1979). The Hellenic arc and trench system: a key to neotectonic evolution of the eastern Mediterranean area, *Tectonophysics*, 60, 1-42.
- McClusky S, S. Balassanian, A. Barka, C. Demir, S. Ergintav, I. Georgiev, O. Gurkan, M. Hamburger, K. Hurst, H. Kahle, K. Kastens, G. Kekelidze, R. King, V. Kotzev, O. Lenk, S. Mahmoud, A. Mishin, M. Nadariya, A. Ouzounis, D. Paradissis, Y. Peter, M. Prilepin, R. Reilinger, I. Sanli, H. Seeger, A. Tealeb, M.N. Toksoz and G. Veis (2000). Global positioning system constraints on plate kinematics and dynamics in the eastern Mediterranean and Caucasus, *J. Geophys. Res.*, 105, 5695-5719.
- McKenzie, D. (1972). Active tectonics of the Mediterranean region, *Geophys. J. Royal Astron. Soc.*, 30, 109-185.
- MacLeod, I.N., K. Jones, and F.D. Ting (1993). 3-D Analytic Signal in the interpretation of total magnetic field data at low magnetic latitudes, *Exploration Geophys.*, 24, 679-688.
- Okay, A.I., I. Isintek, D. Altiner, S.O. Altiner and N. Okay (2012). An olistostrome-mélange belt formed along a suture: Bornova Flysch zone, western Turkey, *Tectonophysics*, 568-569, 282-295.

Determination of buried active faults in Izmir and its surroundings (western Turkey)

- Oruc, B., and E. Balkan (2021). Stress field estimation by the geoid undulations of the Samos-Kusadasi Bay and implications for seismogenic behaviour, *Acta Geophysica*, 69, 3, 1137-1149.
- Papazachos, B.C. and A.A. Kiratzi (1996). A detailed study of active crustal in the Aegean and surrounding region, *Tectonophysics*, 253, 129-153.
- Reilinger, R.E., S.C. McClusky, M.B. Oral, R.W. King, M.N. Toksoz, A.A. Barka, I. Kinik, O. Lenk and I Sanli (1997). Global positioning system measurements of present-day. Crustal movements in the Arabia-Africa-Eurasia plate collision zone, *J. Geophys. Res.*, 102, 9983-9999.
- Rimmele, G., R. Oberhansli, B. Goffe, L. Jolivet, O. Candan and M. Cetinkaplan (2003). First evidence of high-pressure metamorphism in the "Cover Series" of the southern Menderes Massif. Tectonic and metamorphic implications for the evolution of SW Turkey, *Lithos*, 71, 19-46.
- Scordilis, E.M. (2006). Empirical global relations converting Ms and Mb to moment magnitude, *J. Seismol.*, 10, 225-236.
- Sengor, A.M.C. (1979). The North Anatolian Transform Fault: its age, offset and tectonic significance, *J. Geol. Soc. London*, 136, 269-282.
- Sengor, A.M.C. and Y. Yilmaz (1981). Tethyan evolution of Turkey: a plate tectonic approach, *Tectonophysics*, 75, 181-241.
- Sengor, A.M.C., N. Gorur and F. Saroglu (1985). Strike-Slip Faulting and Related Basin Formation in Zones of Tectonic Escape: Turkey as a Case Study, In: Biddle K and Christie-Blick N (Eds) *Strike-Slip Deformation, Basin Formation and Sedimentation*, Special Publications, SEPM Society for Sedimentary Geology, Tulsa, 37, 227-264.
- Spector A and F.S. Grant (1970). Statistical models for interpreting aeromagnetic data, *Geophysics*, 35, 293-302.
- Sozbilir, H., B. Sari, B. Uzel, O. Sumer and S. Akkiraz (2011). Tectonic implications of transtensional supradetachment basin development in an extension-parallel transfer zone: The Kocacay Basin, western Anatolia, Turkey, *Basin Res.*, 23, 423-448.
- Sumintadireja, P., D. Dahrin, and H. Grandis (2018). A note on the use of the second vertical derivative (SVD) of gravity data with reference to Indonesian cases, *J. Engi. Techn. Sci.*, 50, 127-139.
- Tuncer, M.K., N. Oshiman, S. Baris, Z. Kamaci, M.A. Kaya, A.M. Isikara and Y. Honkura (1991). Further evidence for anomalous magnetic structure along the active fault in western Turkey, *J. Geomagn. Geoelectr.*, 43, 937-50
- Uzel, B. and H. Sozbilir (2008). A first record of a strike-slip basin in Western Anatolia and its tectonic implication: The Cumaovasi basin, *Turkish J. Earth Sci.*, 17, 559-591.
- Uzel, B., H. Sozbilir and C Ozkaymak (2012). Neotectonic evolution of an actively growing superimposed basin in western Anatolia: the inner bay of İzmir, Turkey, *Turkish J. Earth Sci.*, 21, 439-471.
- Yadav, P.K., P.K. Adhikari, S. Srivastava, V.P. Maurya, A. Tripathi, S. Singh, R.K. Singh and A.K. Bage (2018). Lithologic boundaries from gravity and magnetic anomalies over Proterozoic Dalma volcanics, *J. Earth Syst. Sci.*, 127, 2.

*CORRESPONDING AUTHOR: Ezgi ERBEK-KIRAN,

Suleyman Demirel University, Faculty of Engineering, Department of Geophysical Engineering Isparta, Turkey

e-mail: ezgierbek@sdu.edu.tr